AD-A032 914 MASSACHUSETTS INST OF TECH CAMBRIDGE FLUID MECHANICS LAB F/G 21/4
A MODEL FOR FUEL-AIR MIXING IN THE TEXACO CONTROLLED COMBUSTION--ETC(U)
JAN 76 B C JAIN, J C KECK, J M RIFE DAAE07-73-C-0282
UNCLASSIFIED FML-76-1 NL

1 OF 1
ADA032914

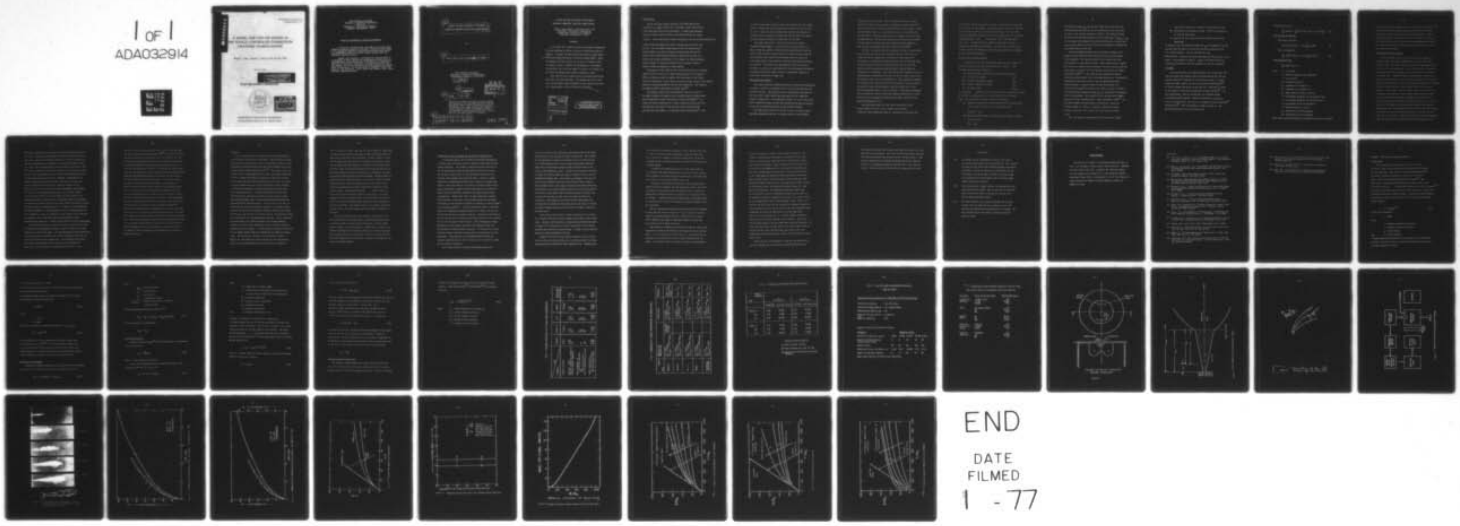

END

DATE
FILMED
1 -77

Fluid Mechanics Laboratory
Publications No. 76-1

A MODEL FOR FUEL-AIR MIXING IN THE TEXACO CONTROLLED COMBUSTION STRATIFIED CHARGE ENGINE

Bhag C. Jain, James C. Keck, and Joe M. Rife

January 1976

FLUID MECHANICS LABORATORY

DEPARTMENT OF MECHANICAL ENGINEERING
MASSACHUSETTS INSTITUTE OF TECHNOLOGY

FLUID MECHANICS LABORATORY
DEPARTMENT OF MECHANICAL ENGINEERING
ROOM 3-252
MASSACHUSETTS INSTITUTE OF TECHNOLOGY
CAMBRIDGE, MASSACHUSETTS 02139

Notice to Recipients of Reprints and Reports

Over the past several years, the number of red-cover Fluid Mechanics Laboratory Reports has declined. This has arisen because of the substantial expense of preparing and mailing reports which will subsequently appear as archival journal articles with substantially identical content.

Reports will continue to be prepared in instances where it is important to record material not appearing in archival form, in instances where rapid dissemination of information is deemed necessary, and in cases where long delays in archival publication are anticipated. To receive preprints of articles submitted to journals prior to publication, you are encouraged to personally contact the Faculty of the laboratory: Profs. Dewey, Fay, Heywood, Keck, Kenyon, Probstein, Shapiro and Sonin.

(6)

A MODEL FOR FUEL-AIR MIXING IN THE TEXACO CONTROLLED COMBUSTION STRATIFIED CHARGE ENGINE

by

(10) Bhag C. Jain, James C. Keck and Joe M. Rife

Fluid Mechanics Laboratory
Department of Mechanical Engineering
Massachusetts Institute of Technology

(12) 49 pp.

(11) January 1976

(14) FML-76-1

Technical and financial support for this research was provided by U.S. Army-Tank Automotive Systems Development Center (Prov) by subcontract to M.I.T from Texaco, Inc., under contracts No. DAAE07-73-C-0282, DAAE07-74-C-0268, and DAAE07-74-C-0168.

(15) DAAE07-73-C-0282
DAAE07-74-C-0268

A MODEL FOR FUEL-AIR MIXING IN THE TEXACO CONTROLLED COMBUSTION STRATIFIED CHARGE ENGINE

Bhag C. Jain, James C. Keck, and Joe M. Rife
Department of Mechanical Engineering
Massachusetts Institute of Technology
Cambridge, Massachusetts 02139

ABSTRACT

A jet model with standard turbulent entrainment assumptions has been developed to predict the spray formation processes in engines. The model has specifically been applied to the Texaco Controlled Combustion System, stratified charge engine. While the analysis has been carried out as part of a general effort to develop a model to predict the performance of the engine, the potential use of the jet model, by itself, as a design tool has also been demonstrated through a parametric study.

Some characteristic lengths useful in evaluating different fuels have also been described. The purpose has been to show that the performance model developed for the engine can be used for a large number of fuels of practical interest.

Introduction

One of the major inputs required for predicting the performance of an engine is the rate of burning of the fuel and the conditions under which this takes place. A simple thermodynamic model can then be used to predict the pressure inside the engine cylinder. These predictions require modelling of the controlling physical processes inside the engine just before, during, and just after combustion. For stratified charge engines with fuel injection and diesel engines, the spray formation processes play the most important role in determining combustion characteristics and, as a result, the overall performance of the engine. An understanding of these processes is therefore essential in developing a model to predict overall performance of these engines.

The purpose of the research work to be described in the following pages has been to carry out a spray analysis as part of the general effort to develop a model to predict the performance of the Texaco Controlled Combustion System (TCCS) stratified charge engines; given engine geometry, operating parameters and the fuel properties. The complete performance model is described in another paper[1].

The analysis begins with the assumption that the process of the spray formation in engines can be studied using continuum models. Such an approach has been used earlier by Rife and Heywood[2] in studies of diesel combustion in a rapid compression machine; and they conclude that the motion of the fuel jet can be satisfactorily analyzed with such models. As reported by Rife and Heywood[2], this

approach assumes that the fuel breaks into droplets near the nozzle orifice and that the relative velocity of droplets in the jet flow is small. They have also concluded that special entrainment assumptions are not required for modelling the fuel jet in an engine so that standard entrainment coefficients can be used.

Our paper starts with a brief description of the TCCS, stratified charge engine. A characteristic lengths analysis is then carried out, partly to determine the applicability of the jet model to this specific engine and partly to determine the range of fuel properties over which the performance model is applicable. A jet model based on the empirical turbulent entrainment parameters is presented. The results of a photographic study of the spray formation to confirm the applicability of the entrainment assumptions are given, and the jet model is used in a parametric analysis to demonstrate its use as a design tool.

TCCS Engine Description

The Texaco Controlled Combustion System, illustrated schematically in Figure 1 requires co-ordination of air swirl, fuel-injection and positive ignition. The high air swirl is obtained by a shrouded inlet valve and is amplified during compression by the combustion chamber configuration. The combustion chamber is a cup in the piston with a cylindrical upper section and toroidal bottom and the diameter of the cup is approximately half of the cylinder diameter.

The high pressure injection system is based on diesel engine injection components and uses a special version of the standard

Roosa Master Pencil Nozzle. The distinguishing feature of this nozzle is a special flat seat and a single-hole orifice instead of the more usual conical seating, multiple-hole sac-tip design. All of the remaining details are essentially the same as a standard production nozzle. Valve opening pressure is usually set in the range of 1500-2000 psi. The positive ignition system specially developed for the engine and called The Texaco Ignition System (TTIS) is a high energy, multi-spark unit with controlled duration[3].

The fuel is injected into the swirling air flow in a downstream direction near the end of the compression stroke. The first increment of fuel is ignited as it reaches the spark plug and a flame-front is established immediately downstream of the spark plug. As fuel injection continues, additional fuel and air reach the flame front at the spark plug and the fuel is burned almost as rapidly as it is injected. For full load,the fuel injection interval approximately corresponds to the time for one air swirl and the overall fuel-air ratio is near stoichiometric. Lower loads are obtained by decreasing fuel injection duration and quantity so that operation is typically lean of stoichiometric and the overall air to fuel ratio may approach 100:1 at idle conditions. These basic conceptual details behind the Texaco Controlled Combustion System are an introduction for our analysis;and additional hardware details can be found in References (4-7).

The performance model for the Texaco stratified charge engine assumes that the rate of chemical heat release during the rapid combustion phase is determined by the mass rate

of injection and the amount of gas mixture entrained by the fuel jet as it reaches the spark plug. This implies that most of the fuel has evaporated by the time it reaches the spark plug. The assumption that the combustible fuel-air mixture at the spark plug is immediately ignited requires that the fuel jet "hit" the spark plug and that mixing in the jet produces combustible fuel-air mixtures in the spark plug vicinity. We will look into the spray formation process to determine the conditions placed on our analysis by these implied assumptions.

Characteristic Length Analysis

A schematic of the spray and various characteristic lengths for the TCCS engine and the fuel spray are shown in Figure 2. The important characteristic lengths are:

(i) Distance between nozzle-tip and spark plug plane L_{sp}

(ii) Jet break-up length L_b

(iii) Droplet deceleration length L_{dec}

(iv) Droplet evaporation length L_{ev}

(v) Momentum length L_{mom}

As suggested previously, our combustion model is applicable if most of the fuel is evaporated by the time it reaches the spark plug plane. For continuum jet models to apply we required:

(a) Rapid jet break-up and droplet deceleration occuring within a few orifice diameters or "at the nozzle tip".

$$L_b, L_{dec} \ll L_{sp}$$

(b) Most of the fuel must be evaporated by the time it reaches the spark plug.

$$L_{ev} \simeq L_{sp}$$

The momentum length L_{mom} defines the length scale over which the momentum introduced into the jet by entrainment of the cross flow is equal to the initial momentum of the jet. The momentum length determines the relative bending of the jet centerline. If $L_{mom} << L_{sp}$, we can neglect the bending of the jet centerline due to cross flow; otherwise, the effects of cross flow must be included in studying the space-time history of the jet.

The relationships between the characteristic lengths, fuel properties and injection system parameters have been established in the appendix. The various characteristic lengths have been calculated for a wide range of fuels. These characteristic lengths have then been compared with the distance between nozzle-tip and the spark plug to ascertain the relationships required for our simple performance model[1]. The types of fuels considered include methanol, gasoline, diesel and a wide-range distillate. The physical properties of these fuels used in the calculations have been listed in Table 1 and the results of the calculations, the characteristic lengths for each of the fuels, are given in Table 2. The characteristic geometric length L_{sp} for the present arrangement is $\tilde{\sim}$ 1.5 centimeters. On the basis of our characteristic lengths analysis, we have concluded that a single performance model[1] can be used to predict the performance of the Texaco engine for a large number of fuels of practical interest including methanol, gasoline, JP-4, diesel and a wide-range distillate since;

(a) The injection velocities used in practice are higher

than those required for "immediate" break-up of the jet.

(b) Deceleration of droplets is rapid - within a millimeter or so from the nozzle tip.

(c) Most of the fuel evaporates by the time it reaches the spark plug.

In addition since the momentum length and L_{sp} are comparable, we also conclude that the effect of cross-flow has to be included in the jet mixing analysis. We now desctibe the jet model used to calculate the space-time history of the fuel jet in the engine. This analysis is used to compute the amount of gas entrained by the fuel jet and the trajectory of the jet centerline.

Jet Model:

From the characteristic lengths analysis, we conclude that the fuel jet breaks into droplets near the nozzle orifice and that the relative velocity of droplets in the jet flow is small. A quasi-steady jet model, similar to the one used by Rife and Heywood[2] is used to analyze the motion of the fuel jet. The model is based on the turbulent entrainment assumptions of Hoult and Weil[8]. In this analysis,the rates of entrainment for turbulent plumes introduced by Hoult and Weil have been modified to include the effects of large density variations, as suggested by Ricou-Spalding[9] and Escudier[10]. The jet geometry is shown in Figure 3. The governing equations for the jet motion are:

Conservation of Mass:

$$\frac{d}{ds}\left(\rho\pi b^2 u\right) = \left(\frac{\rho}{\rho_\infty}\right)^{1/2} 2\pi b\rho_\infty \left[\alpha|u - V_t| + \beta|V_n|\right] \qquad (1)$$

Conservation of Momentum:

Horizontal component:

$$\frac{d}{s}\left(\rho\pi b^2 u^2 \cos\theta\right) = V \cos\phi \frac{d}{ds}\left(\rho\pi b^2 u\right) \qquad (2)$$

Vertical Component:

$$\frac{d}{ds}\left(\rho\pi b^2 u^2 \sin\theta\right) = V \sin\phi \frac{d}{ds}\left(\rho\pi b^2 u\right) \qquad (3)$$

Conservation of Fuel:

$$\frac{d}{ds}\left(\rho\pi b^2 u\, x_f\right) = 0$$

where b = jet radius

s = distance along the jet trajectory

u = jet velocity

V = cross-flow velocity

V_n = component of V normal to u

V_t = component of V parallel to u

x_f = mass fraction of fuel in the jet

α = entrainment parameter for the parallel flow

β = entrainment parameter for the normal flow

θ = inclination of jet to horizontal

ρ = mixture density in the jet

ρ_∞ = density of the surrounding gas

ϕ = inclination of V to horizontal

With these governing equations, the problem reduces to an initial

value problem and knowing the initial conditions of the fuel jet and the nature of the cross-flow, the equations can be numerically integrated to obtain the space-time history of the jet. Before using this model to obtain the rates of entrainment and the space-time history of the jet; a number of spray photographs were taken in a high pressure bomb to determine the character of our nozzle and verify the jet model.

Photographic Studies of Spray:

A block diagram of the system used is shown in Figure 4. A variable speed motor (Range 0-1600 RPM) was used to drive the injection pump. The motor also had a variable trigger signal unit mounted on it which could give a signal before start of injection. This signal was used to trigger an oscilloscope with a variable time-delay unit. A delayed trigger signal from the oscilloscope triggered the driving unit for the micro-flash system. [The driving unit for the micro-flash could also be triggered manually if desired.] The micro-flash unit gave a very intense flash of microsecond duration. The original unit was modified from a line source with a parabolic reflector to a point source and a Fresnel lens was used to obtain uniform intensity throughout the field of view. Various diffusers and aperture settings were used to reduce the intensity of the light at the film plane to prevent over-exposure. Nitrogen was used to pressurize the vessel and a small flow through the vessel was maintained during injection to scavege the fuel vapor out of the vessel to improve resolution of the jet boundaries. Fuel was injected horizontally to prevent the splashing on the

plexiglas windows that occurred when vertically downward injection was used. A number of photographs with different delay times were taken for each set of operating conditions to study the history of the jet development and to compare it with the predictions of the jet model. The cracking pressure for the injector was set at ≈ 100 atmospheres (1500 psi) and ambient densities in the pressure vessel of up to 16.5 atmospheres were used. The variable speed motor and the injection pump were driven at ≈ 640 RPM, corresponding to an engine speed of approximately 1280 revolutions per minute, and various injection rates were used. While few details in the interior of the jet can be seen in these photographs; the boundary of the jet as it developed with time was very clearly visible. Interior details could not be seen within the jet because of the high droplet density within the jet; relatively high jet velocities; the presence of large amounts of fuel vapor within the pressure vessel; and poor quality of plexiglas windows. A typical set of photographs is shown in Figure 5. The photographs are for an ambient density of 16.5 atmospheres, close to conditions in the chamber at the beginning of injection, and a fuel flow rate of approximately 35 cubic millimeters per injection. Diesel fuel was used for all the photographs.

The tip position and the radius of the jet as a function of time was measured from photographs similar to those in Figure 5 and this data was to test the jet model. The spreading angle and jet radius were measured and used to calculate the value of entrainment parameter 'α' in the jet model in these computations. The photographs were taken in a quiescent atmosphere and the value of the entrainment coefficient β was not tested. The entrainment parameter 'α' was

observed to be approximately 0.08 which compares very well with the value of 0.11 used by Hoult and Weil[8] and we have chosen to use their entrainment coefficients of $\alpha = 0.11$ and $\beta = .6$. We conclude from the photographs, that the assumptions required for a continuum computation are appropriate and that classical entrainment parameters can be tused. To determine the appropriate value for the initial jet radius, the jet model was used to compare measured and computed penetration-time history of the fuel jet and two different cases were considered. In one, the scaling parameter, effective initial jet radius, was assumed to be equal to the orifice size with a coefficient of discharge equal to 1.0. In the other case, the discharge coefficient of 0.61 for a sharp-edged orifice was used to get the effective initial jet radius and the initial momentum of the jet. The predictions of the jet model were then plotted in the form of jet radius and tip position as a function of time and compared against the actual values obtained from the photographs. As can be seen from Figures 6 and 7, a discharge coefficient of 0.61 gives reasonably good agreement between the theoretical predictions and experimental data. This step is important, since the flat seating orifice used in this engine is quite different from the sac tip nozzle used by Rife and Heywood. In these calculations, an effective initial jet radius of 0.0223 centimeters has been used for an orifce of 0.0288 centimeters.

Analysis

The jet motion has been studied in a two dimensional plane containing the nozzle and the spark plug. The gas velocity inside the cylinder has been assumed to be a solid-body rotation and the magnitudes of this solid body swirl have been obtained from a gas-motion analysis carried out by Martin[11]. The nozzle orifice is assumed to be a "sharp-edged orifice" with a discharge coefficient of 0.61 to obtain the effective initial jet radius and two different mean values of initial momentum have been used - one based on time-averaged mass rate of flow (total mass of fuel injected per injection divided by the injection duration) and the other time averaged momentum. A third limiting case has also been considered where the injection pulse is assumed to be a square wave with its height equal to the maximum injection velocity obtained during the injection pulse. For this case, it is also assumed that the injection duration changes to vary engine output and that the mass rate of injection remains constant at all loads. The density ratio used for rate-of-entrainment calculations is based on the conditions at the beginning of injection. In our studies,we have found that a jet velocity based on the average momentum appears to yield the most appropriate results with the injection system used on this engine. The calculations have been carried out for two engine speeds, 1500 and 2500 RPM and for light and medium loads. The initial jet velocities used are given in Table 3. Typical jet centerlines are shown in Figure 8, and the gas-fuel ratios at the spark plug for all cases are shown in Figure 9.

It is seen that, in most cases, the distance between the spark plug and the jet-center line is less than or equal to the jet radius so that the jet will "hit" the spark plug. In this context, it must also be noted that while the jet is assumed to be symmetric about the centerline for the analysis, in practice, the cross-flow will probably result in a skewed distribution ensuring the "hitting" of the spark plug in all cases for the present arrangement of spark plug location and injection and swirl matching. Figure 9 shows the gas-fuel ratio at the spark plug. As can be seen, while the load conditions affect centerline trajectory, the gas to fuel ratio at the spark-plug plane is almost independent of both the load and the speed. This favorable system occurs because an increase in initial momentum enhances the entrainment from the tangential relative velocity vector but reduces the time for the fuel to reach the spark plug plane resulting in less entrainment from the cross-flow. The overall result is an almost constant gas to fuel ratio at the spark plug over a wide range of initial jet momentum.

The results obtained from this analysis, specifically the gas-to-fuel ratio at the spark plug, can be used directly in the performance model to compute engine performance. The jet model itself, however, can also be used as a design tool to predict the effects of changes in the injection system, air swirl or the spark plug location relative to the nozzle. Some of the predictions of this model along with a discussion of its uses as a design tool are given in the next section.

Predictions of the Jet Model and Its Uses as a Design Tool:

As explained above, the jet model was primarily designed to calculate input parameters for the combustion model under present design conditions. For example, computed space-time history of the jet demonstrates that the spark plug is "hit" by the spray and the gas to fuel ratios at the spark plug location are combustible under present operating conditions. However, a major objective in developing this model is to construct a design tool which can adequately predict the effects of design changes on the engine performance, suggest possible improvements and clearly indicate various trade-offs involved in any design changes under consideration. Having shown that the model adequately explains the development of the spray under present design and operating conditions, we now proceed to examine the effects of certain changes in the design conditions. We will use the jet model to study the effects of changing one design parameter at a time on the jet trajectory and the rate of growth of the jet. We will use the value of gas-to-fuel ratio at the present spark plug location as the indicator of the rate of growth of the fuel jet. After changing one design parameter, we will always come back to the present design conditions before changing another parameter. In the process, we will look for various trade-offs involved and the possibilities for improvements. The parameters to be changed include initial jet velocity, magnitude of air swirl, density ratio, initial jet radius and the angle of injection.

Let us first look at a typical relationship between the

gas-to-fuel ratio at the spark plug and the location of the spark plug relative to the injector as shown in Figure 10. The location of the spark plug relative to the nozzle can be an effective way for controlling the rate of heat release during rapid combustion phase and a relationship similar to Figure 10 will exist in all cases in this parametric study. Values of the parameters required as inputs for the jet model are listed in Table 4 for the case of 2500 RPM and medium load. Also listed are changes in the value of each of the parameters that have been studied in this analysis. These changes cover a wide range of potential operating conditions. The effects on the rate of growth of the jet as seen by the gas-to-fuel ratio at the present spark location are given in Table 5 and trajectories for many of these cases are shown in Figures 11 through 13. The trajectory is plotted in the common plane containing both the nozzle and the spark plug and all figures include the present design locations of the injector (origin), spark plug and their axis.

As we can see from Table 5, a large variation in the initial jet velocity causes only a small change in the value of gas-to-fuel ratio. However, the trajectory is significantly affected as shown in Figure 11; and because the relative magnitudes of the initial momentum and cross-flow momentum change - a larger initial velocity results in reduced bending of the jet.

Changes in the swirl rates greatly influence the gas-to-fuel ratio at the spark plug; because the cross-flow is about six times more efficient in entrainment than tangential flow. Remember that

the tangential entrainment parameter $\alpha = 0.11$ and the cross flow $\beta = 0.6$. The effect on the trajectory as shown in Figure 12, is a result of a change in the relative magnitudes of initial momentum and the cross-flow momentum or, stated differently, in the momentum length.

A change in the density ratio has a small effect both on gas-to-fuel ratio and trajectory with a reduction in the density ratio slightly increasing the gas-to-fuel ratio at the spark plug and a small increase in the bending of the jet.

A change in the effective initial jet radius significantly affects both the trajectory and the gas-to-fuel ratio. Note that trajectory scales directly with the initial radius so that on a dimensionless diagram of the jet centerline, the trajectory does not change. A smaller initial jet radius gives an increased value of the gas-to-fuel ratio at the plug and increased bending of the jet centerline.

The jet centerline resulting from various values of the angle of injection are shown in Figure 13. A zero angle of injection implies vertically downward injection normal to the air swirl. Such a change in the angle of injection sharply increases the gas-to-fuel ratio as shown in Table 5.

The parametric analysis just described brings out some of the trade-offs involved in the design of the injection system and the engine. It also demonstrates a technique for testing possible improvements in the design for better overall performance of the engine. For example, one of the ways to improve the performance

and the maximum power rating of this engine is to improve its volumetric efficiency by reducing the requirement of air swirl. Clearly, a reduction in swirl will affect both the gas-to-fuel ratio and the trajectory. While a change in the jet centerline trajectory can be compensated for by moving the spark plug, we have also concluded that any reduction in the gas-to-fuel ratio at the spark plug will adversely affect the engine performance. Thus, we would like to reduce the swirl and, at the same time, maintain the gas-to-fuel ratio at the spark plug at least as high as the present value. Our parametric analysis shows that this goal can be achieved: by moving the spark plug farther away from the nozzle tip; or by reducing the nozzle orifice size; or by reducing the angle of injection with respect to cylinder axis; or by a combination of any of these changes. Thus, given a new value of the swirl rate, we can calculate the changes required in other parameters and the new location of the spark plug which will compensate the effect of reduction in the swirl and build gas-to-fuel ratio as desired. As another example, consider a reduction in the initial velocity of the fuel jet. Such a reduction would permit us to work with lower injection pressures. We have shown that such a change would have a rather small effect on the gas-to-fuel ratio, and therefore, gas-to-fuel ratio considerations do not constrain the value of initial velocity to any great extent.

These are just a few examples to show that the model can be uses as a design tool in evaluating various possibilities for

improvements in either the design of the injection system or in the performance of the engine. Of course, in many such cases, the model will only give partial information and other considerations - like physical limitations in bringing the spark plug and the injector closer or in changing the angle of injection etc., will enter the picture. But the utility of the model as a design tool is clear.

Conclusions

(i) An analysis of the development of spray in the Texaco stratified charge engine has been carried out. The analysis is based on a jet model with standard turbulent entrainment assumptions. While the analysis is specifically for the TCCS engine; we believe that the model is general enough to be applicable to diesel engines and stratified charge engines using fuel injection.

(ii) Some characteristic lengths useful in evaluating different fuels have been described. Most of the fuels of practical interest have been shown to satisfy our criteria for a simple engine performance model.

(iii) The spray analysis can be used as a design tool to gain insight into some important fuel injection, swirl rate matching and combustion characteristics of the engine. We have illustrated our claim with a parametric analysis using jet model.

ACKNOWLEDGMENTS

The authors are thankful to Professors Heywood and Hoult of M.I.T., Mr. Ed Mayer of Texaco and Mr. Walter Bryzik of USATACOM for their help in this work. Technical and financial support for this research was provided by U.S. Army Automotive Systems Development Center (Prov) by subcontract to M.I.T. from Texaco,Inc., under contracts No. DAAE07-73-C-0282, DAAE07-74-C-0268, and DAAE07-74-C-0168.

References

(1) Jain, B.C., and Keck, J.C., "A Performance Model for the Texaco Controlled Combustion, Stratified Charge Engine," Fluid Mechanics Laboratory Report No. 76-2, January 1976.

(2) Rife, J. and Heywood, J.B., "Photographic and Performance Studies of Diesel Combustion with a Rapid Compression Machine," SAE paper 740948.

(3) Canup, R.E., "The Texaco Ignition System - A New Concept for Automotive Engines," SAE paper 750347.

(4) Davis et al., "Fuel Injection and Positive Ignition - A Basis for Improved Efficiency and Economy," Paper 190A presented at SAE Summer Meeting, Chicago, June, 1960.

(5) Mitchell, et al., "Design and Evaluation of a Stratified Charge Multifuel Military Engine," SAE Transactions, Vol. 77 (1968), paper 680042.

(6) Mitchell et al., "A Stratified Charge Multifuel Military Engine - A Progress Report," SAE Paper 720051.

(7) Alperstein et al., "Texaco's Stratified Charge Engine - Multifuel, Efficient, Clean and Practical," SAE Paper 740563.

(8) Hoult, D.P., and Weil, J.C., "Turbulent Plume in a Laminar Cross Flow," Atmospheric Environment, Vol. 6, 1972, pp. 514-531 (Printed in Great Britain).

(9) Ricou, J.P., and Spalding, D.B., "Measurement of Entrainment by Axial Symmetric Turbulent Jets," J. Fluid Mech., 9,21 (1961).

(10) Escudier, M.P., "Aerodynamics of a Burning Turbulent Gas Jet in a Cross Flow," Combustion Science & Technology, April, 1972.

(11) Martin, M.K., S.M. Thesis, Mech. Engineering, M.I.T. (1975).

(12) Haenlein, A., "On the Disruption of a Liquid Jet," Forsch Arb. Geb. Ing. Wes. 1931, Vol. 2, (#4, April).

(13) Weber, C., "On the Disruption of a Liquid Jet," Z. Angew. Math. Mech. 1931, Vol. 11, (#2, April).

(14) Ohnesorge, W.V., "The Formation of Drops from Nozzles and the Disruption of a Stream of Liquid," Z. Angew. Math. Mech., 1936, Vol. 16 (#6, December).

(15) Burt and Troth, "Penetration and Vaporization of Diesel Fuel Sprays," Diesel Engine Combustion, Inst. Mech. Engrs., 1969-70, paper #15.

(16) Beer, J.M., and Chigier, N.A., "Combustion Aerodynamics," John Wiley and Sons, 1972.

(17) Ranz, W.E., and Marshall, W.P., "Evaporation from Drops," Chem. Eng. Progress, 48, pp 141-146 and 173-180 (1952).

Appendix: Characteristic Lengths Analysis

Jet Break-up:

It is generally recognized that there are several different modes of jet breaking-up depending upon the velocity of the fluid jet. Four modes were identified by Haenlein[12] including "complete and immediate disruption of the jet". Other modes were analyzed mathematically by Weber[13] but there is no treatment by either Haenlein or Weber of this mode. A similar definition of atomization modes was stated by Ohnesorge[14] along with empirically defined dimensionless numbers to predict the boundaries between the different modes. He defines the mode boundaries by relating a number Z characteristic of the fluid to the Reynolds number Re, where

$$Z = \eta/(\sigma\rho_f d)^{1/2} \qquad \text{(A-1)}$$

and for mode boundaries

$$Z = Z(Re)$$

where

η = absolute viscosity of the fluid

σ = surface tension of the fluid

ρ_f = liquid density

and d = nozzle diameter

A simple dimensional analysis of the important forces (neglecting gravity) will show that the two relevant dimensionless numbers are the Weber Number $We = \rho V^2 d/\sigma$

and the Reynolds Number $Re = \rho Vd/\eta$

The characteristic number Z can be formed for these two dimensionless groups by eliminating velocity.

The minimum Reynolds number for immediate disruption is then given by Ohnesorge in terms of a power law

$$Z = c(Re)^n \qquad \text{(A-2)}$$

where

$$n = -1.26$$

$$c = 1096$$

So that for immediate and complete break-up (i.e. $L_b << L_{sp}$):

$$Re \geq 259/Z^{0.8} \qquad \text{(A-3)}$$

This correlation is based on dimensional analysis and has been verified by Burt and Troth[15]. The characteristic number Z can be calculated given fluid properties and the nozzle orifice size. Substituting this into Equation (A-3); we can establish the minimum Re for immediate disruption of the jet for the given fluid.

Deceleration of Droplets

Equating the change in momentum of the droplet to the aerodynamic drag force, we can give the characteristic deceleration time as:

$$\tau_{dec} \simeq D_{drop}(\rho_f/\rho_a) \; / \; C_d \, V_{initial} \qquad \text{(A-4)}$$

where

D_{drop} = droplet diameter

ρ_f = fluid density

ρ_a = air density

C_D = coefficient of drag

$V_{initial}$ = initial velocity of the droplet relative to air

The corresponding deceleration length then is

$$L_{dec} = \tau_{dec} \times V_{initial} = D_{drop}(\rho_f/\rho_a)/C_D \qquad \text{(A-5)}$$

and for the model to be applicable

$$L_{dec} << L_{SP}$$

Droplet Vaporization

Based on Beer and Chigier[16], the characteristic vaporization time can be given as

$$\tau_{ev} \simeq D^2_{drop}/\lambda \qquad \text{(A-6)}$$

where λ is the evaporation constant.

For a single stagnant drop in an infinite atmosphere, the evaporation constant λ_s is given as:

$$\lambda_s = 8\ k\ \ln\ (1 + B)/\rho_f\ C \qquad \text{(A-7)}$$

where

$B = C(Tg-Ts)/Q$ = Transfer number

Q = latent heat of vaporization and sensible heat to raise droplet temperature to boiling point

Tg = mean gas temperature

Ts = droplet surface temperature

ρ_f = density of the fuel

C = specific heat of air

and k = thermal conductivity of air

A number of phenomena excluded by the assumption of a "single stagnant drop in an infinite atmosphere" can modify the evaporation rate of a droplet and the most important is the forced convective motion of the gas relative to the droplet. The effect of this phenomenon is included on the basis of a correlation given by Ranz and Marshall[17] for Reynolds number between 0 and 200 and low values of B.

$$\lambda = \lambda_s (1 + 0.30\ Sc^{1/3}\ Re^{1/2}) \qquad \text{(A-8)}$$

where Sc = Schmidt number of the gas (equal to the ratio of momentum transfer to the mass transfer)

$$Sc = \mu_\infty / \rho_\infty D \qquad \text{(A-9)}$$

and the Reynolds number (Re) is

$$Re = \rho_\infty \ U_\infty D_{drop}/\mu_\infty \qquad \text{(A-10)}$$

where ρ_∞ and μ_∞ are the density and viscosity of the gas far upstream from the droplet; D is the diffusion coefficient and U_∞ is the gas velocity relative to the droplet. In our case, for droplets of about ten micron size, the above correlation gives $(\lambda_i/\lambda_s) \sim$ 10-11 where λ_i is based on the initial jet velocity. Since the actual case is somewhere in between, we will take

$$\lambda = (\lambda_i+\lambda_s)/2 \simeq 6\lambda_s \qquad \text{(A-11)}$$

Equations (A-6), (A-7), and (A-11) with the knowledge of mean droplet diameters can be used to calculate a characteristic length of vaporization. We will require that it be less than or comparable to the distance between nozzle tip and spark location so that almost all of the fuel is vaporized by the time it reaches the spark plug.

$$L_{ev} \lesssim L_{SP}$$

Momentum Length Considerations

The momentum length defines the length scale over which the sum of the momentum flux of the cross-flow across the jet boundary becomes equal to the initial momentum of the jet. This will determine

whether the bending of the spray axis must be included in the analysis. From Hoult and Weil[8] and Escudier[10] the momentum length is:

$$L_{mom} = [\rho_o u_o^2 b_o^2 / \rho_\infty V^2]^{1/2} \qquad \text{(A-12)}$$

where ρ_o = initial density of the liquid jet

u_o = initial velocity of the jet

b_o = initial radius of the jet

ρ_∞ = density of the cross-flow

V = velocity of the cross-flow

Table 1: PHYSICAL PROPERTIES OF THE FUELS UNDER CONSIDERATION

Property \ Fuel	Methanol	Gasoline	JP-4	Diesel	Wide-Range Distillate
Chemical Formula	CH_3OH	(C_8H_{16})		$(C_{12}H_{26})$	
Density, gm/cc	0.796	0.76	0.77	0.82	0.785
Absolute Viscosity, centipoise	0.46	0.40	0.89	3.61	50
Surface Tension, dynes/cm	21	20	21	23	21.5
Boiling Range, ^0C					
Initial Boiling Point		40	60	200	43
50%	65	100	160	275	181
Final Boiling Point		200	250	350	324
Heat of Vaporization, cal/gm	262	64	50	39	55
Lower Heating Value					
per unit mass, cal/gm	4,794	10,260	10,340	10,420	10,500
per unit volume, cal/cc	3,806	7,798	7,962	8,544	8,243

Table 2: CHARACTERISTIC LENGTH CONSIDERATIONS FOR VARIOUS FUELS

Length / Fuel	Break-up and Deceleration		Vaporization	Momentum
Methanol	$Z = 0.0047$ Rey. $\geq$ 18,860 $V_{initial} \geq 1{,}920$ cm/sec	~150 drop diameter ~1.5 mm	$B = 0.386$ $\lambda_s = 1.96 \times 10^{-4}$ cm^2/sec $\tau_{ev} = 0.85$ msec	$L_{mom} > L_{sp}$ [but not very large]
Gasoline	$Z = 0.0043$ Rey. $\geq$ 20,255 $V_{initial} \geq 1{,}900$ cm/sec	"	$B = 1.032$ $\lambda_s = 4.46 \times 10^{-4}$ cm^2/sec $\tau_{ev} = 0.34$ msec	$L_{mom} \simeq L_{sp}$
JP - 4	$Z = 0.0093$ Rey. $\geq$ 10,930 $V_{initial} \geq 2{,}220$ cm/sec	"	$B = 0.772$ $\lambda_s = 3.55 \times 10^{-4}$ cm^2/sec $\tau_{ev} = 0.47$ msec	$L_{mom} \simeq L_{sp}$
Diesel	$Z = 0.0348$ Rey. $\geq$ 3,800 $V_{initial} \geq 3{,}000$ cm/sec	"	$B = 0.39$ $\lambda_s = 1.92 \times 10^{-4}$ cm^2/sec $\tau_{ev} = 0.87$ msec	$L_{mom} \simeq L_{sp}$
Wide-Range Distillate	$Z = 0.51$ Rey. $\geq$ 444 $V_{initial} \geq 4{,}962$	"	$B = 0.639$ $\lambda_s = 3.01 \times 10^{-4}$ cm^2/sec $\tau_{ev} = 0.55$ msec	$L_{mom} \simeq L_{sp}$

Table 3 : INITIAL JET VELOCITIES FOR SPRAY ANALYSIS

Volume Injected / RPM	20 mm^3/inj		45 mm^3/inj	
	$\dot{q}$ mm^3/CA°	velocity,cm/sec	$\dot{q}$ mm^3/CA°	velocity,cm/sec
1500 (1)	1.80	10,387	2.67	15,365
(2)	1.10	6,354	2.00	11,553
(3)	3.50	20,140	3.50	20,140
2500 (1)	1.21	11,553	1.88	18,099
(2)	1.00	9,627	1.67	16,077
(3)	2.75	26,475	2.75	26,475

Initial Momentum based on

(1) Time averaged momentum

(2) Time averaged mass rate of flow

(3) Square wave with maximum injection velocity

Table 4: LIST OF INPUTS FOR PARAMETRIC ANALYSIS USING JET MODEL

Present Operating Conditions at 2500 RPM, 45 mm^3 fuel/injection

Initial Jet Velocity	= 18, 100 cm/sec
Swirl-Solid Body Rotation	= 10 x Engine Speed
Density Ratio-Fuel-to-gas	= 85
Effective Initial Jet Radius	= 0.02227 cm
Angle of Injection	= 34°

Range of Values for Parametric Analysis

Parameter	Range of Values				
Initial Jet Velocity, cm/sec	6,000	12,000	18,100	24,000	30,000
Swirl-Solid Body Rotation (times engine speed)	0	5	10	15	20
Density Ratio	45	65	85	105	125
Effective Initial Jet Radius, cm	0.005	0.01	0.02227	0.04	0.06
Angle of Injection, degrees	0	17	34	51	68

[Zero angle implies vertically down injection].

Table 5 : PREDICTIONS FROM PARAMETRIC ANALYSIS USING JET MODEL

GAS-TO-FUEL RATIO AT THE PRESENT SPARK PLUG LOCATION

Parameter	Value of the Parameter	Gas To Fuel Ratio
Initial Jet Velocity	6,000 cm/sec	9:1
	18,100	10.6:1
	30,000	10:1
Swirl	0 x Engine Speed	4:1
	10	10.6:1
	20	15:1
Density Ratio	45	13.3:1
	85	10.6:1
	125	9.5:1
Effective Initial Jet Radius	0.005 cm	17:1
	0.02227	10.6:1
	0.060	6:1
Angle of Injection	0 degrees	17:1
	34	10.6:1
	68	5:1

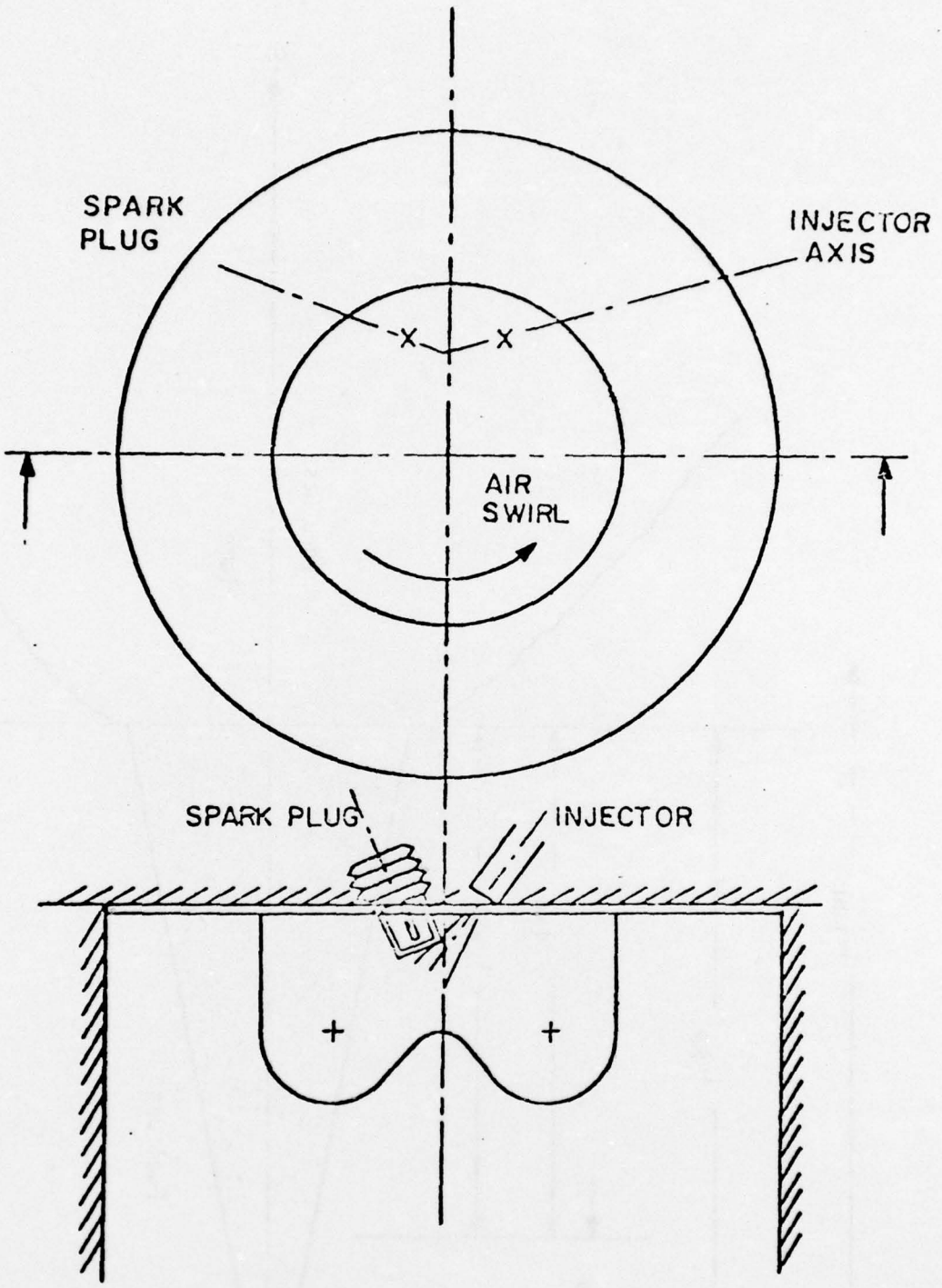

TEXACO CONTROLLED COMBUSTION
SYSTEM (SCHEMATIC)

Figure :1

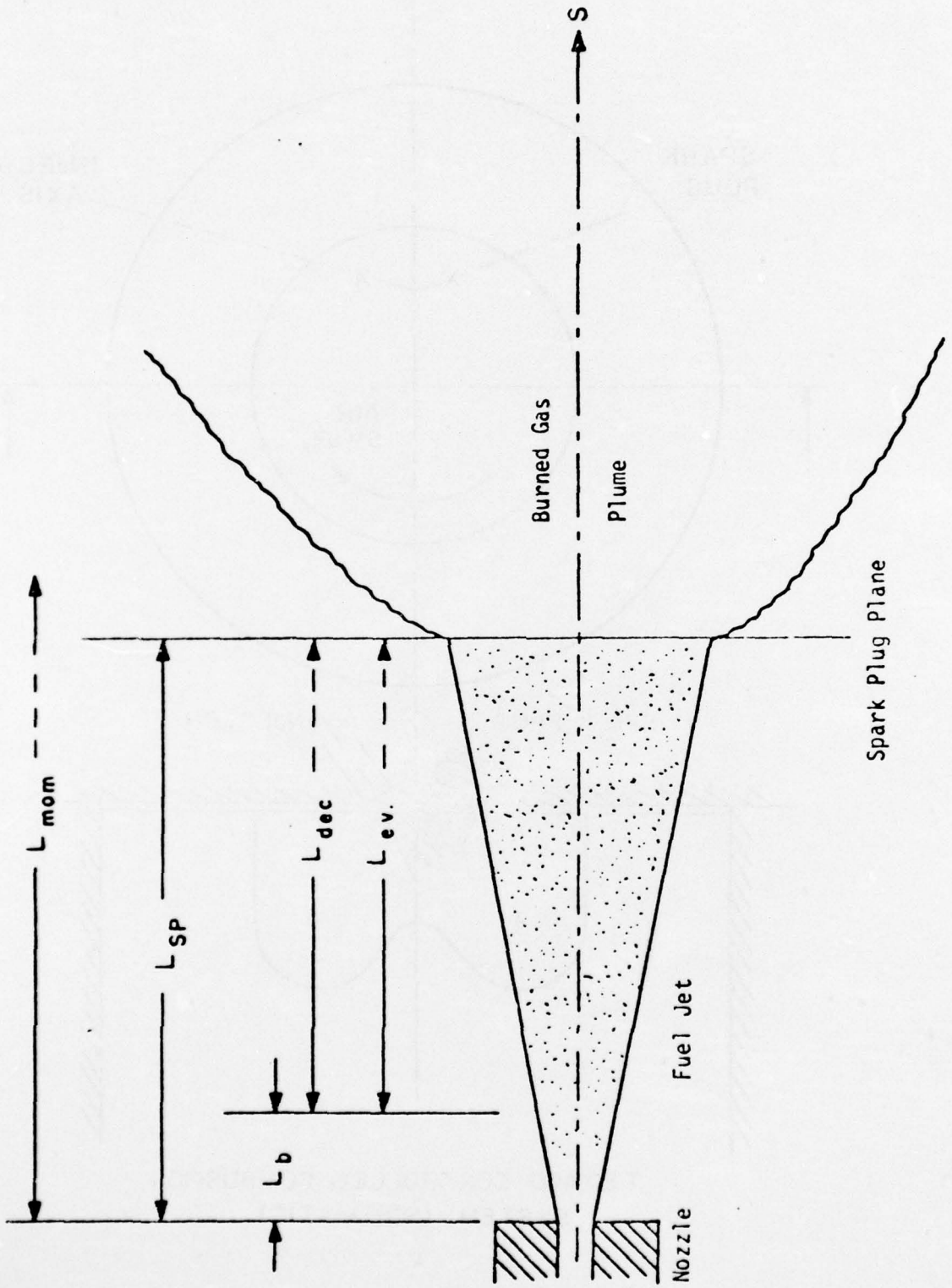

Figure 2: Spray Schematic and Characteristic Lengths

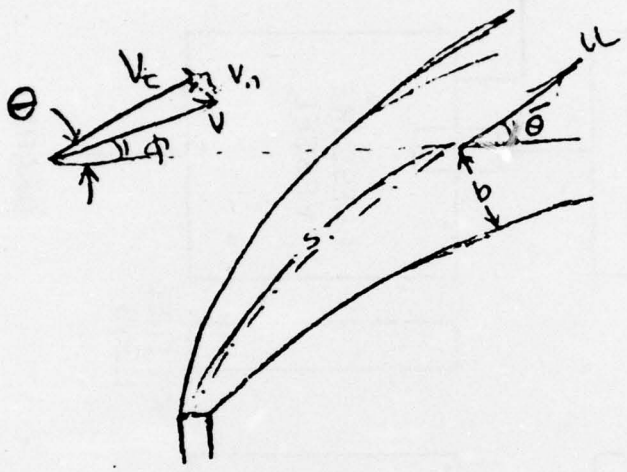

Figure 3: Geometry of the Jet

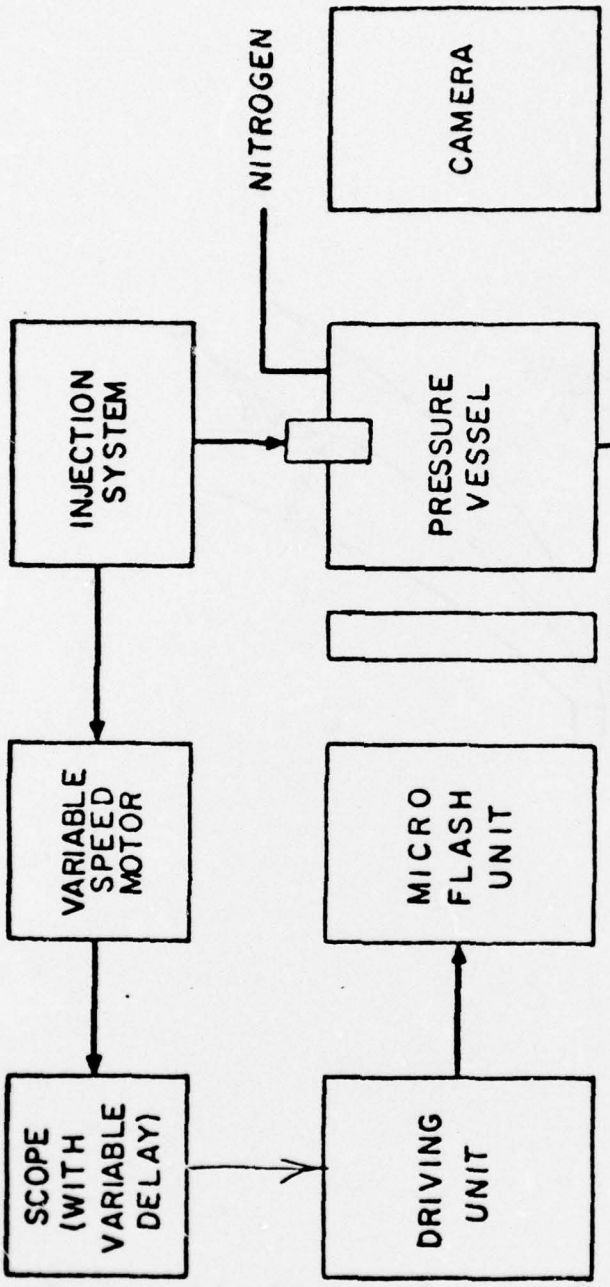

Figure 4 : System for Spray Photography-Block Diagram

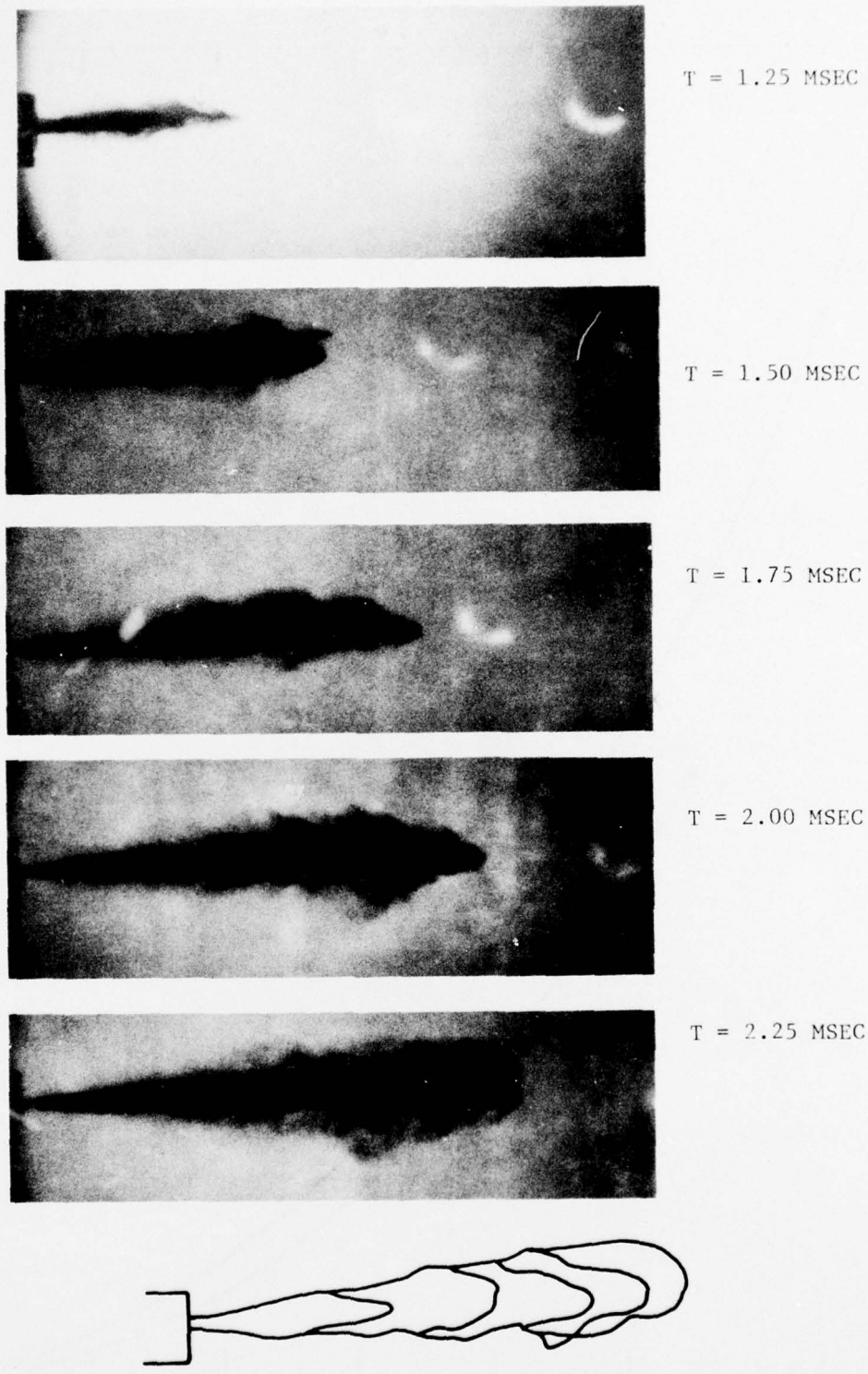

Figure 5: Photographs of the development of spray
Ambient density: 16.5 atmospheres, Scale:
Nozzle diameter = 0.9 cm.

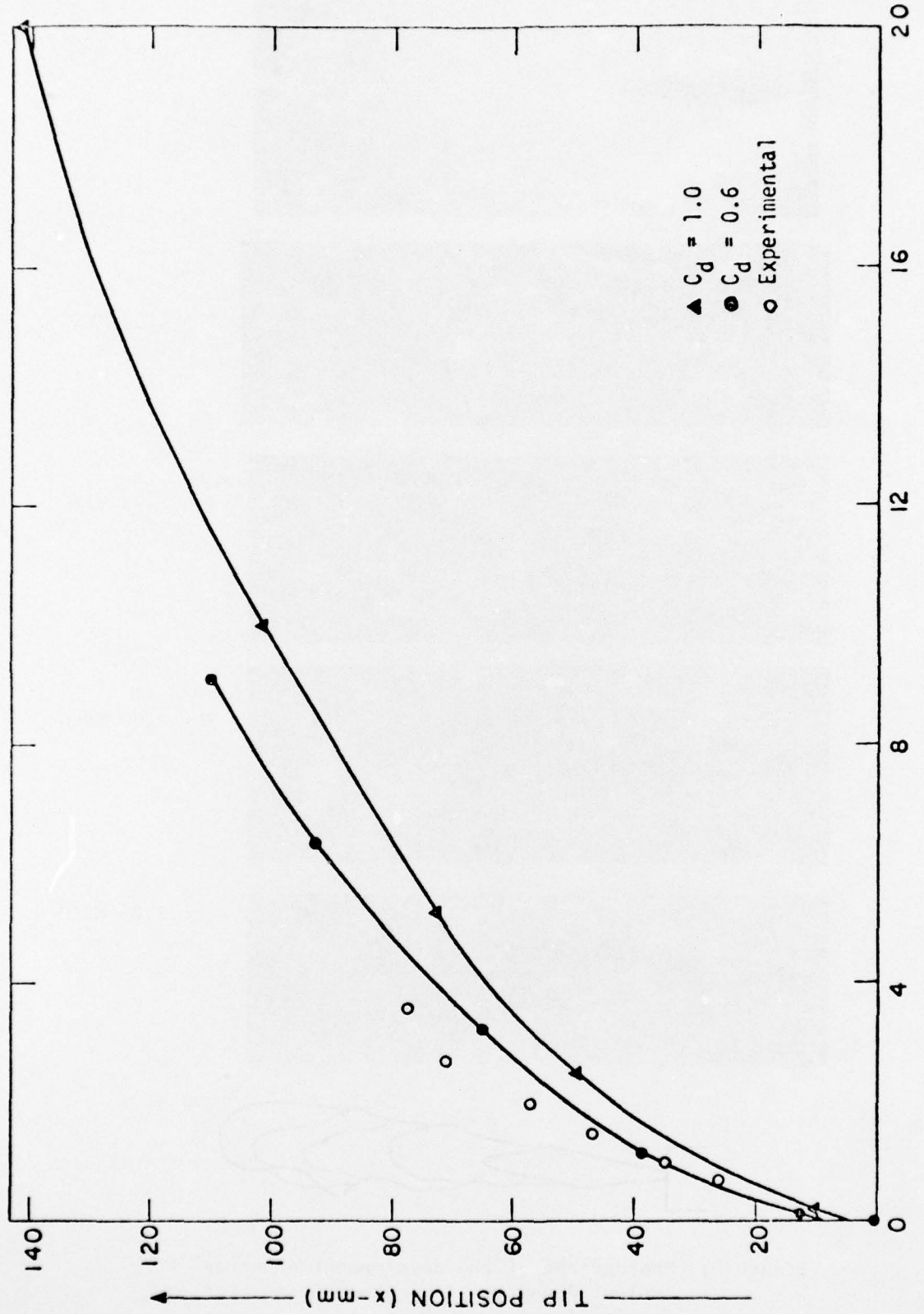

Figure 6 : Determination of Effective Initial Jet Radius - Tip Position Vs. Time

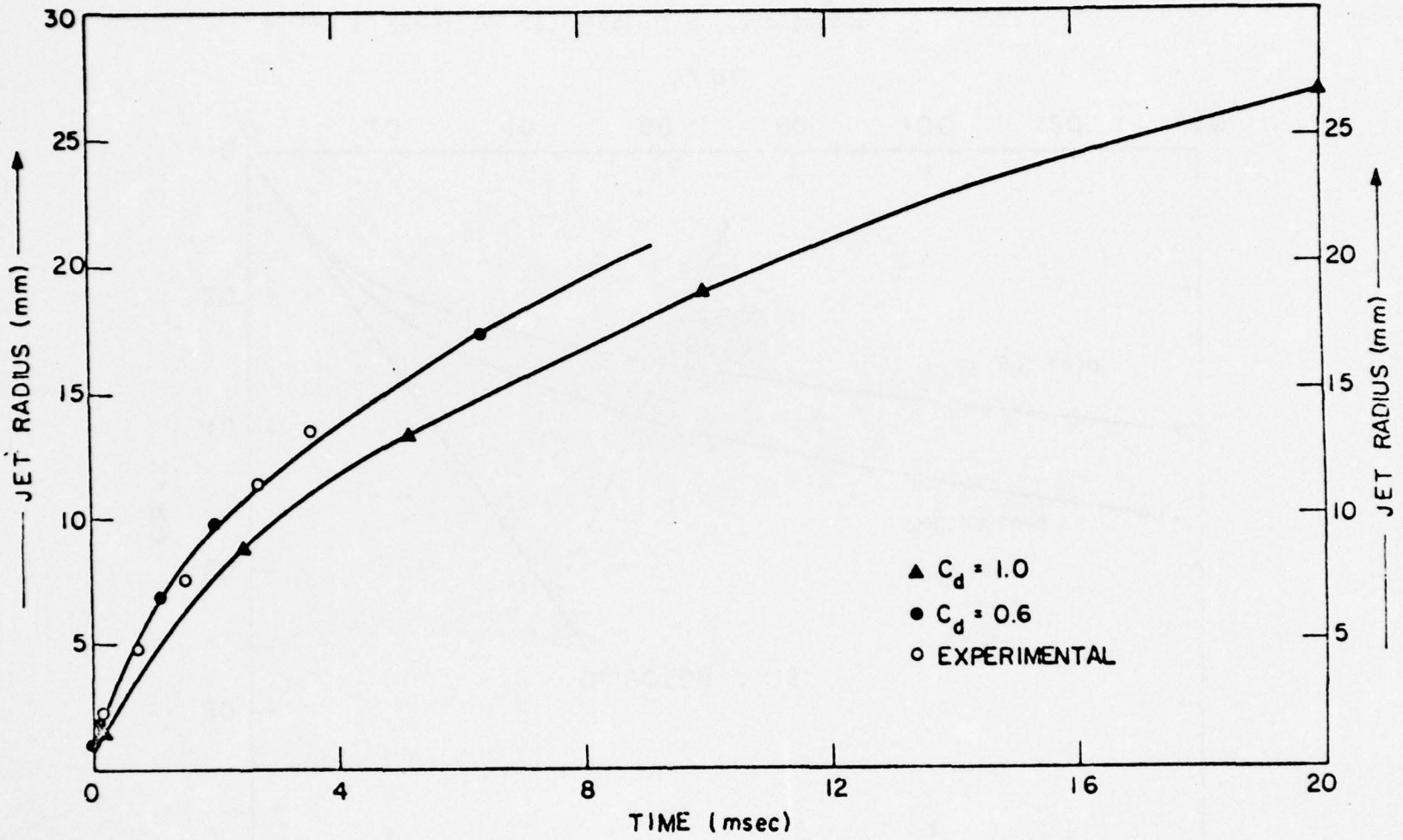

Figure 7.: Determination of Effective Initial Jet Radius - Jet Radius Vs. Time.

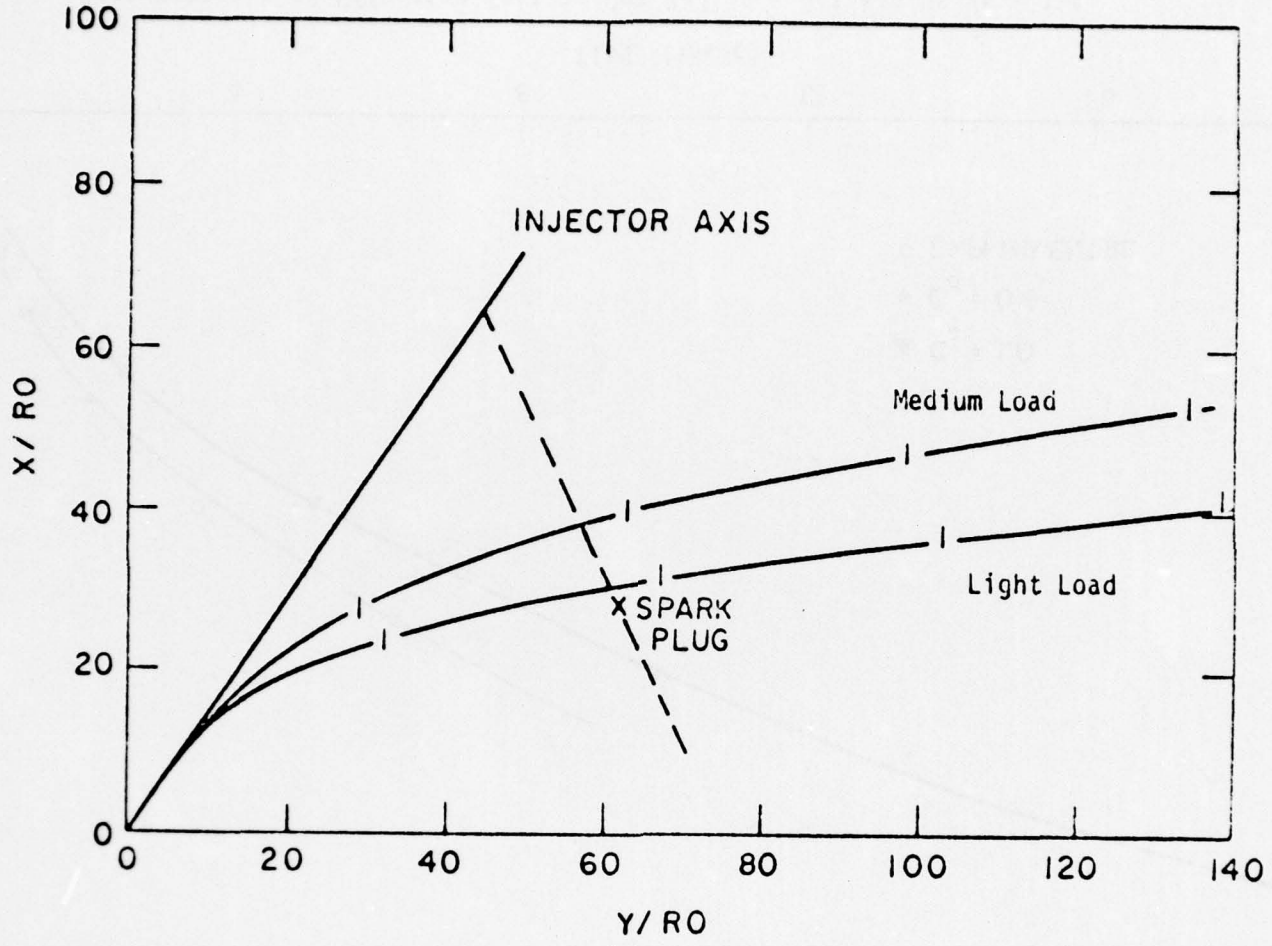

Figure 8: Predicted Jet Centerline Trajectories

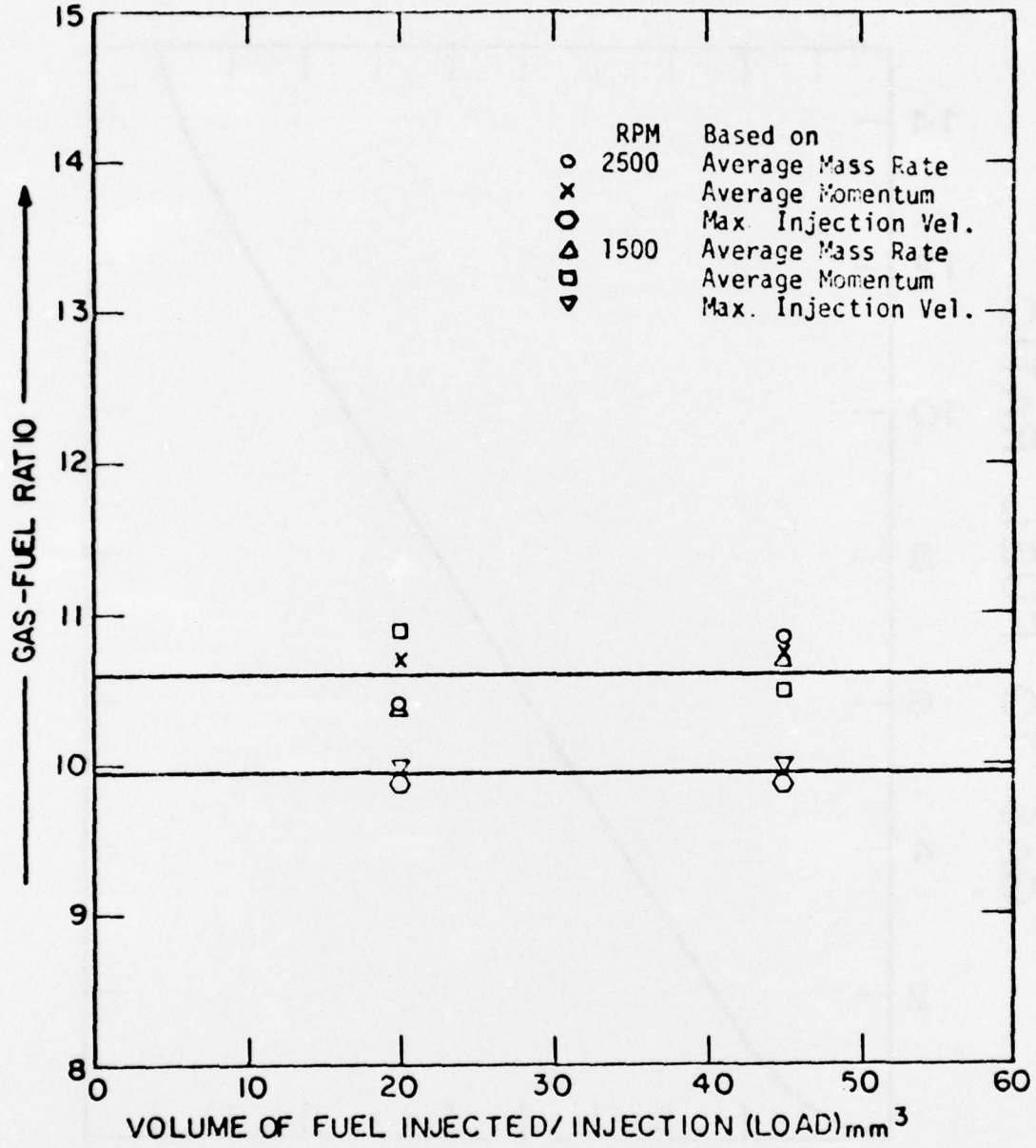

Figure 9: Predicted Gas-To-Fuel Ratios for Present Design Conditions.

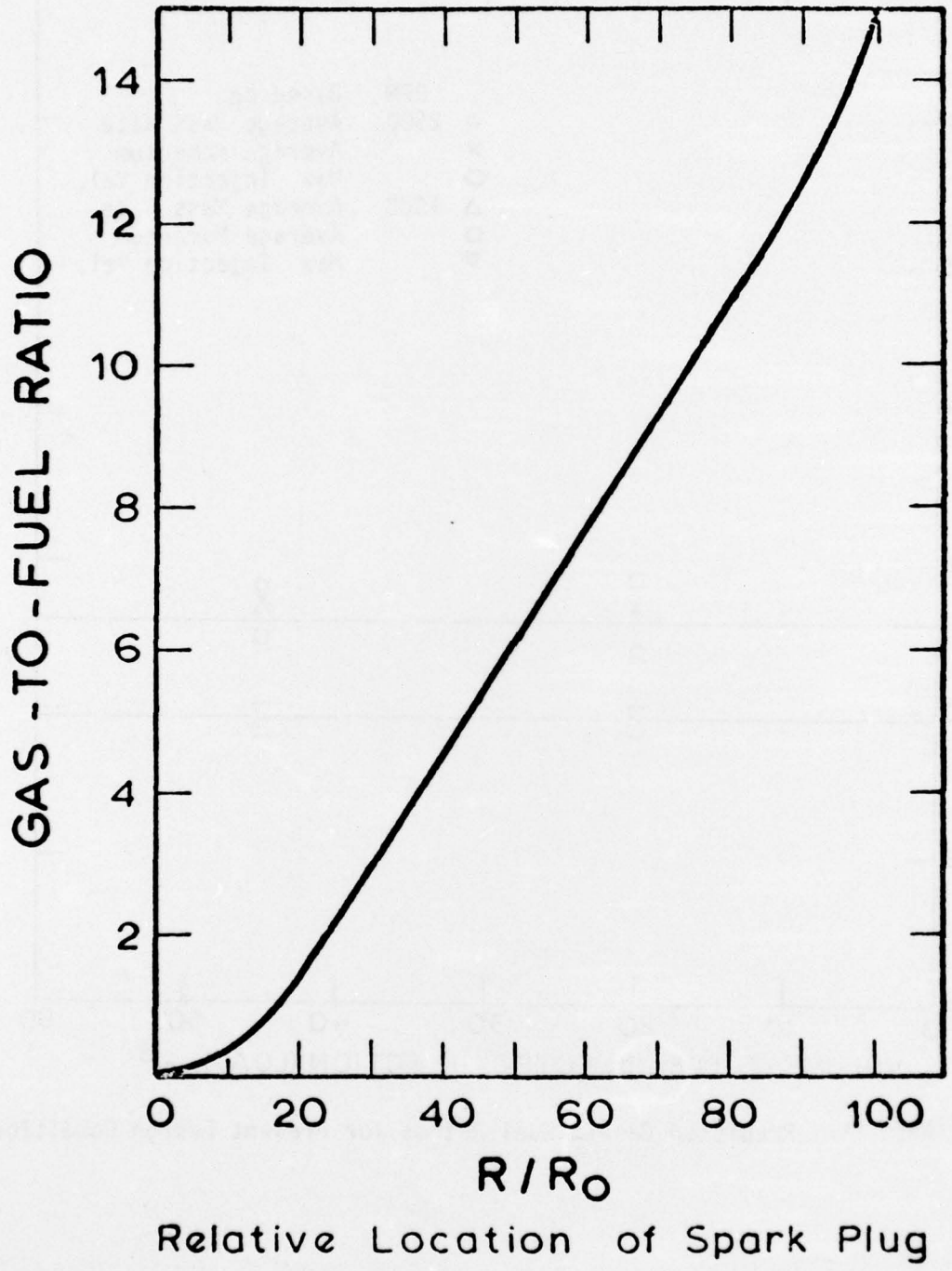

Figure 10: Effect of relative spark location on gas-to-fuel ratio

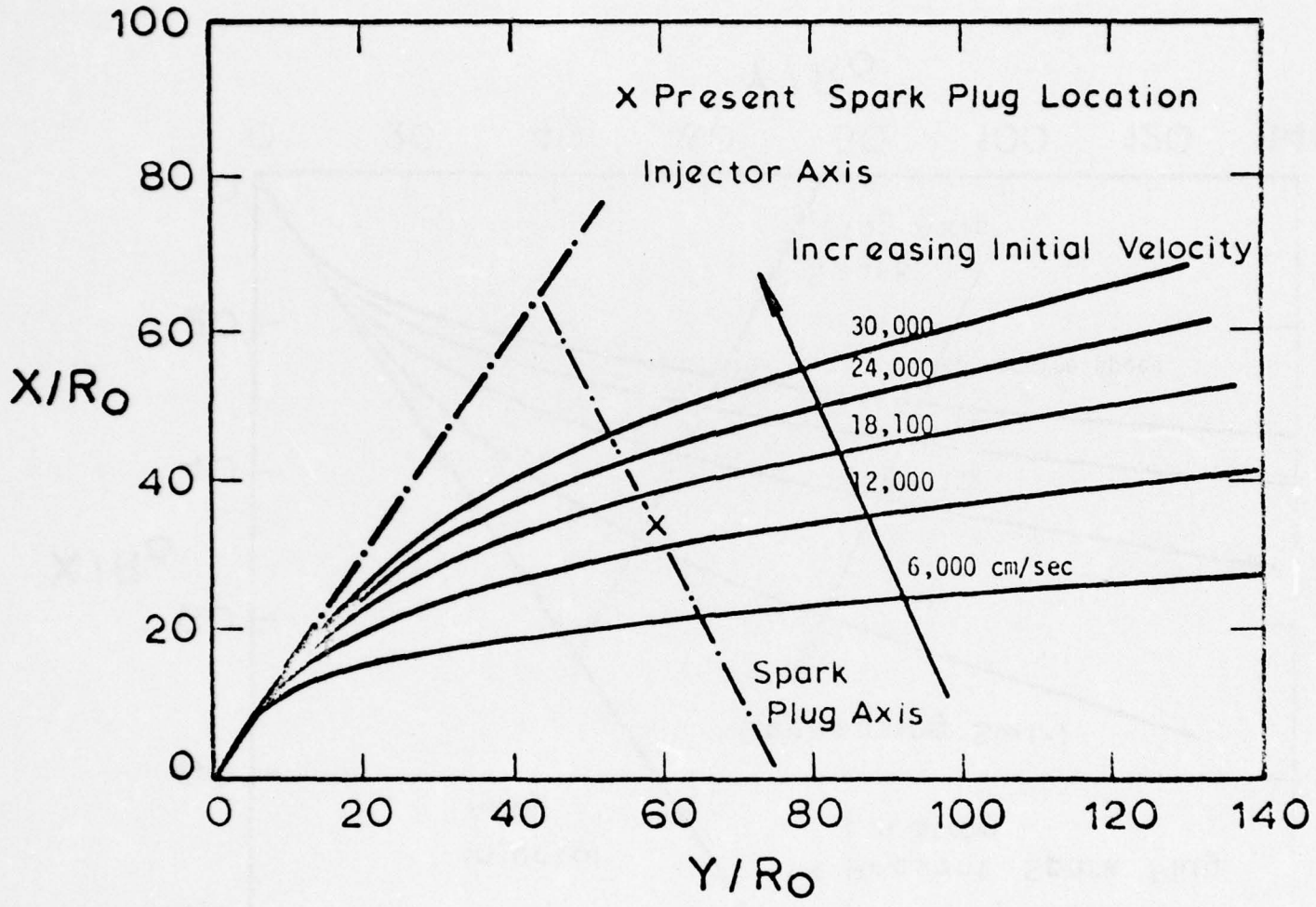

Figure 11: Effect of initial jet velocity on jet trajectory

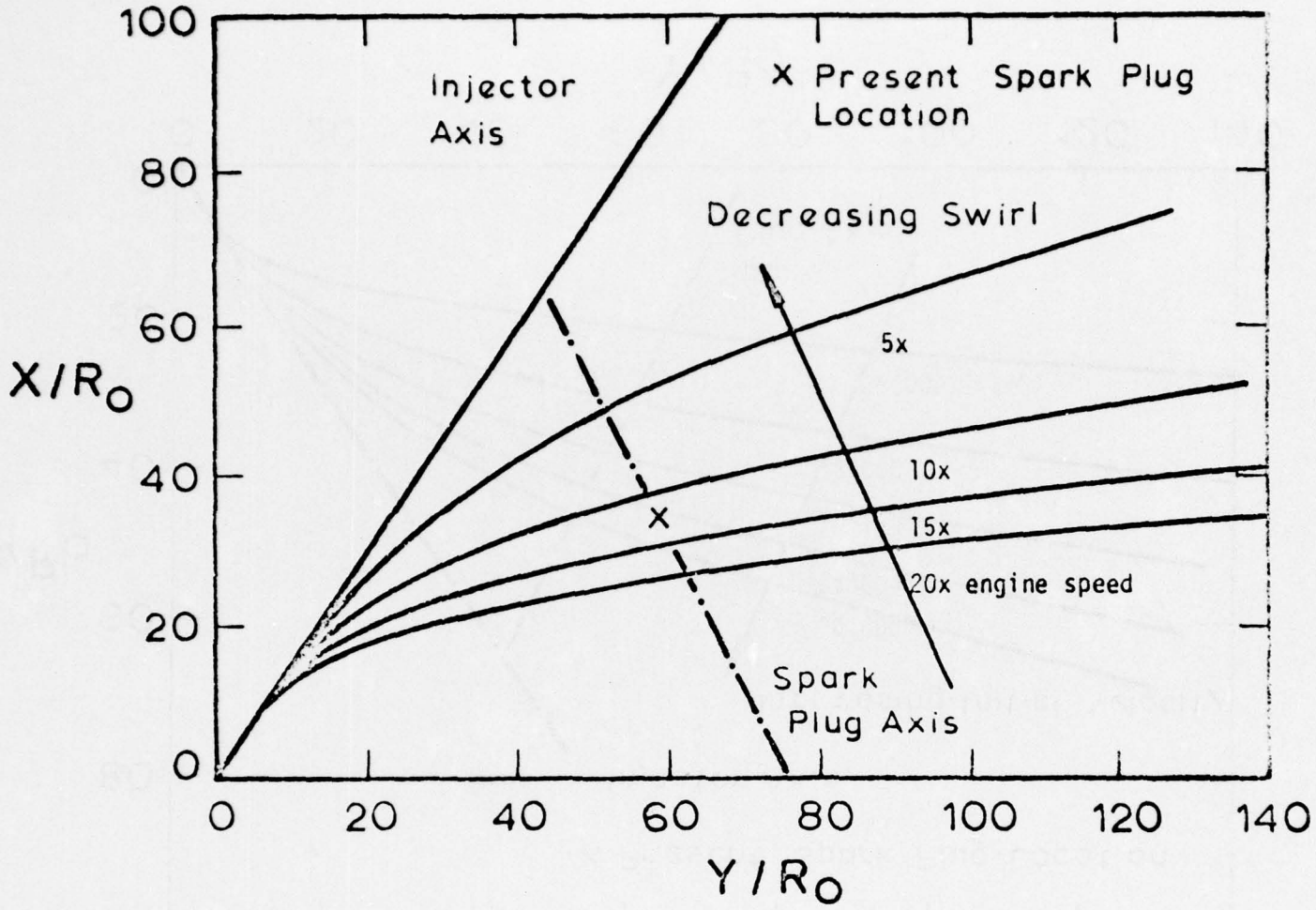

Figure 12: Effect of Swirl on jet trajectory

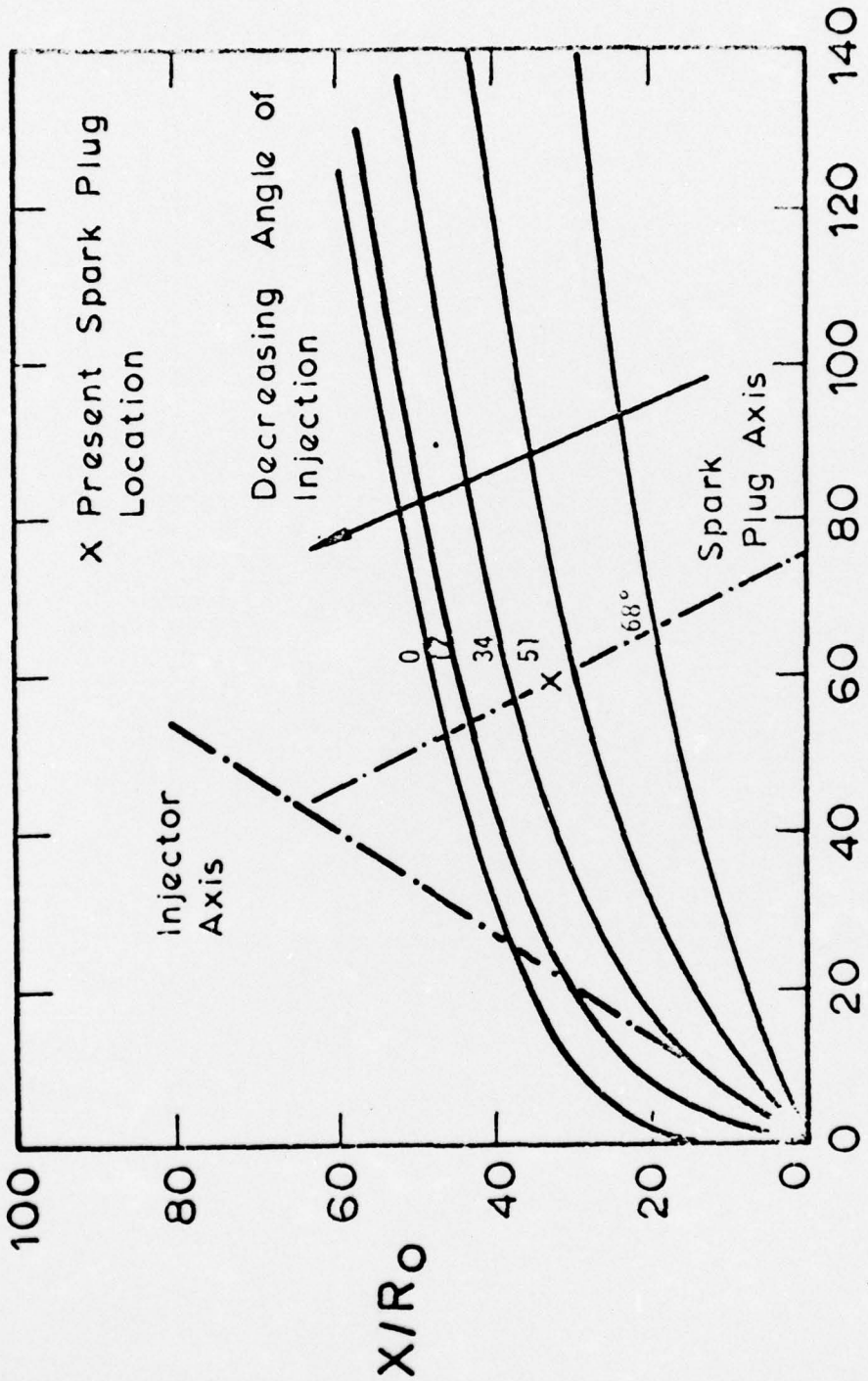

Figure 13: Effect of angle of injection on jet trajectory